An Ultrasound Imaging and Computational Fluid Dynamics Protocol to Assess Hemodynamics in Iliac Vein Compression Syndrome

Ismael Z. Assi,[a] Sabrina R. Lynch, PhD,[a] Andrea T. Obi, MD,[b] Krystal Samulak, RPhS RVS,[b] David M. Williams, MD,[c] Thomas W. Wakefield, MD,[b] C. Alberto Figueroa, PhD[a,b]

[a] From the Department of Biomedical Engineering, University of Michigan; [b] Section of Vascular Surgery, Department of Surgery, University of Michigan Health System; [c] Division of Interventional Radiology, Department of Radiology, University of Michigan Health System

To be submitted to: Journal of Vascular Surgery – Venous and Lymphatic Disorders

Conflicts of Interest and Source of Funding: None of the authors report conflicts of interest.

Corresponding Author: Ismael Assi

Email: ismael@umich.edu

Phone: 734-763-8680

Address: 2800 Plymouth Rd Building 20-210W, Ann Arbor, MI 48109

Keywords: Iliac Vein Compression Syndrome, May-Thurner Syndrome, Computational Fluid Dynamics, Deep Vein Thrombosis, Ultrasound Imaging, Non-thrombotic Iliac Vein Lesion

Article Highlights

Type of Research: Protocol for a single center, prospective, non-randomized, case-control study.

Key Findings: A protocol was developed to measure venous hemodynamics via ultrasound, create 3D models of the iliac veins using CT and ultrasound, and compute blood shear rates in iliac veins using computational fluid dynamics. Preliminary analyses have revealed that Iliac Vein Compression Syndrome patients may experience shear rates higher than 1000 s^{-1}.

Take Home Message: This paper presents a standardized method to study Iliac Vein Compression Syndrome shear rates using computational fluid dynamics, CT, and ultrasound.

Table of Contents Summary

A protocol combining ultrasound, CT, and computational fluid dynamics was developed to assess shear rates in the iliac veins. Analyses revealed that Iliac Vein Compression Syndrome patients may experience shear rates higher than 1000 s^{-1}. Elevated shear rates may play a role in deep vein thrombosis in these patients.

Abstract

Objective: Elevated shear rates are known to play a role in arterial thrombosis; however, shear rates have not been thoroughly investigated in Iliac Vein Compression Syndrome patients due to imaging limitations and assumptions on the low shear nature of venous flows. This study was undertaken to develop a standardized protocol to quantify Iliac Vein Compression Syndrome shear rates.

Methods: Eligible patients have their iliac vein hemodynamics measured via duplex ultrasound. Two of the following three vessel locations are required: IVC, RCIV, and LCIV; in addition to acquiring data at the REIV and LEIV. Ultrasound velocity spectra are multiplied by a weighted cross-sectional area of ultrasound (US) and CT data to create flow waveforms. Flow waveforms are then scaled to ensure conservation of flow is maintained in the IVC and common iliac veins. A 3D, patient-specific model of the iliac vein anatomy is constructed from CT and ultrasound. Flow waveforms and the 3D model are used as a basis to run a computational fluid dynamics simulation (CFD). Flows in internal iliac veins and cross-sectional areas of the common iliac veins are iteratively calibrated due to collateral vessel flow and discrepancies between CT and US area measurements. Simulation results on mean velocity are validated against ultrasound data at measurement locations. Simulation results are post-processed to derive spatial and temporal values of quantities such as velocity and shear rate.

Results: Preliminary analyses (N=2) have revealed that Iliac Vein Compression Syndrome patients experience elevated shear rates, with some shear rates reaching over 1000 s^{-1}.

Conclusions: We developed a protocol that obtains hemodynamic measurements of the inferior vena cava and iliac veins from ultrasound, creates patient-specific 3D reconstructions of the venous anatomy using CT and ultrasound, and computes shear rates using calibrated CFD

methods. Preliminary results have indicated that Iliac Vein Compression Syndrome patients experience elevated shear rates. Further studies are needed to assess the relationship between vein compression and shear rates in Iliac Vein Compression Syndrome patients compared to controls with non-compressed iliac veins.

Body

Introduction

Iliac Vein Compression Syndrome (IVCS), formerly known as May-Thurner Syndrome, is an anatomical variant in which the right common iliac artery compresses the left common iliac vein (LCIV) against the lumbar spine[1]. IVCS is associated with an increased risk of deep vein thrombosis (DVT)[2]. Despite IVCS being prevalent in 20% of the population[1], much remains unclear about the association of IVCS and DVT.

The three broad categories that contribute to DVT pathogenesis, as described by Virchow's Triad, are alterations in blood flow, endothelial injury, and hypercoagulability[3]. Venous stasis from decreased LCIV flow and endothelial damage from arterial pulsations have been proposed as potential mechanisms for the occurrence of DVT in IVCS patients[4,5]. Furthermore, hypercoagulability is associated with risk factors such as hormonal changes, COVID-19, genetic causes such as Factor Leiden V, shear activation of platelets and more[6,7]. One hypercoagulable risk factor that has been overlooked in IVCS is shear activation of platelets, which is often considered as a main contributor to thrombosis initiation in the arterial system[8]. Shear activation of platelets in the arteries typically begins to occur at shear rates around 1000 s^{-1} and is known to contribute to thrombosis initiation by increasing platelet-platelet adhesion[8,9]. However, due to the venous circulation being regarded as a low shear system, blood shear rate has not been thoroughly investigated thus far as a potential thrombotic mechanism in IVCS patients.

Venous shear rates are less well understood than their arterial counterparts, due to challenges with visualizing the deeper veins using routine imaging and with obtaining reliable and reproducible velocity measurements due to breathing and vessel motion artefacts. The tool most frequently used to assess venous hemodynamics is ultrasound (US). Ultrasound scans are highly dependent on the operator and patient body habitus[10]. Furthermore, standard US measures velocity at a given section of the vessel, and assumptions on circularity are made to extrapolate values of flow[11]. Shear rates can then be approximated by dividing average ultrasound velocities by the vessel radius. This approach, however, provides a single value of shear rate for the entire vessel and is therefore a significant oversimplification.

One tool that can provide insight on quantities not easily accessible *in vivo* is CFD, a well-established technique that uses numerical analysis to solve the equations that describe fluid motion (known as the Navier-Stokes equations). CFD provides high-resolution 3D descriptions of velocity, shear rate, and pressure in complex geometries and has been used extensively to assess arterial hemodynamics[12,13] and to assist in surgical planning[14–16].

Challenges in obtaining reliable venous geometry and hemodynamic data, together with the collapsibility of the vessels, have all contributed to the relatively sparse deployment of CFD methods on the venous circulation. Thus, the lack of established venous computational modeling practices motivates the need for a well-designed, controlled research study of venous shear rates in IVCS patients, which is the purpose of this protocol.

Methods

Study Design and Eligibility Criteria

This is a single-center, non-randomized study conducted at the Diagnostic Vascular Unit (DVU) at the University of Michigan Health System, a large regional hospital with expertise in venous diseases. The study has been approved by the University of Michigan institutional review board as IRB-HUM00212189. **Figure 1A** depicts the basic protocol components, which lead to the estimation of blood shear rate in the iliac veins. **Figure 1B** summarizes the ultrasound data acquisition. The study population consists of patients aged 18 years or older with IVCS and DVT and/or lower extremity symptoms (Subject group) or with peripheral arterial disease and no IVCS compression (Control group). These patients were selected as controls due to the readily available CT data, thereby only requiring venous hemodynamic assessment via ultrasound at the DVU. Subjects or Controls are excluded from the study if they do not have a recent CT scan on file, if the CT scan is of insufficient quality, or if the iliac veins cannot be well visualized on ultrasound.

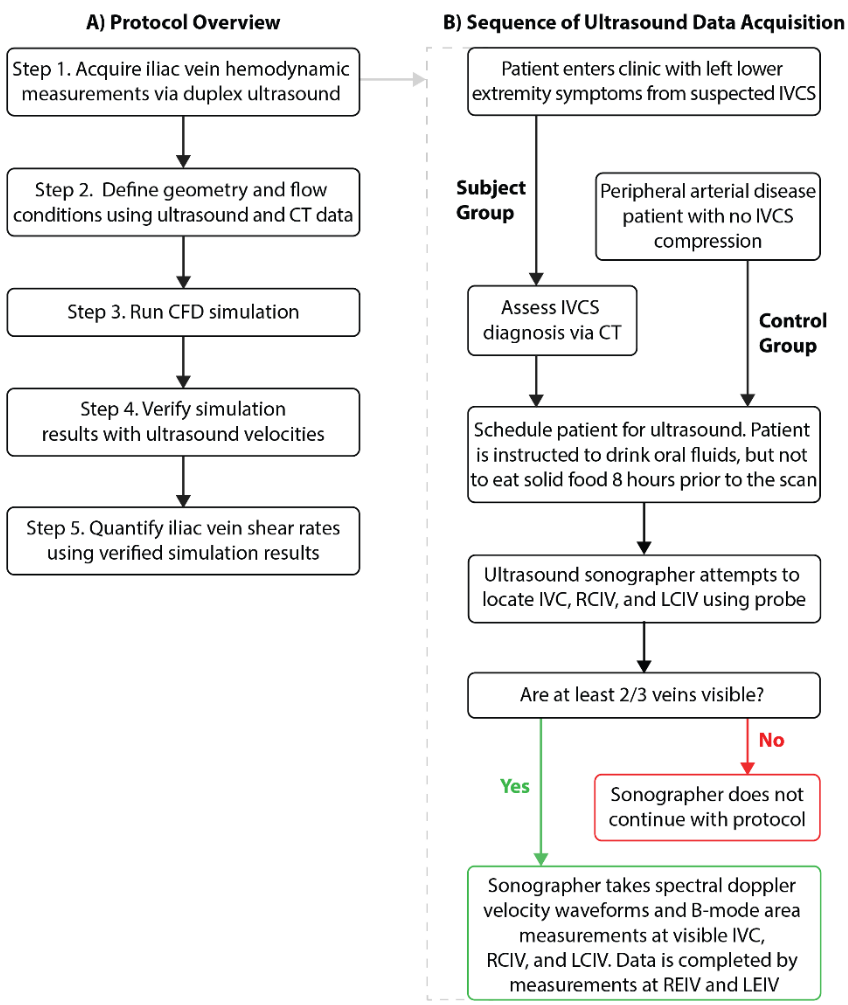

Figure 1. (A) The protocol is outlined by 5 key steps. (B) Once a Subject or Control has been identified as a study candidate, they are scheduled for an ultrasound scan. If the sonographer can visualize at least 2 out of 3 key locations, velocity and area measurements are acquired via duplex ultrasound.

Computed Tomography

An abdominal and pelvic CT scan is performed following intravenous iodinated contrast injection. For optimal opacification of the pelvis and abdomen, images are taken 2 minutes after contrast injection. This allows the contrast to reach the slow-filling veins[17]. CT scans performed at the University of Michigan follow standard delayed phase procedures.

Ultrasound Protocol

Patient preparation: Duplex ultrasound is commonly used to evaluate venous bilateral lower extremities for deep and superficial venous thrombosis[18]. To improve visualization of the inferior vena cava (IVC) and common iliac veins, patients are instructed to drink oral fluids, but not to eat solid food for at least 8 hours prior to the scan. All ultrasound measurements are taken in the supine position to standardize gravitational effects on areas calculated from US and CT. Patients are instructed to breathe normally during US scans. Prior to the scan, the sonographer measures patient respiratory rate. All US imaging in this study is performed with the GE Logiq E9 system and a C1-6 probe. The probe's target angle is 60 degrees or less.

Obstruction assessment: To rule out obstruction, venous lower extremity B-mode and spectral doppler with distal augmentation US scans are performed by taking a dual image with and without compression[19].

Velocity and area assessment: Data acquisition is divided into two parts. First, the sonographer attempts to visualize the IVC, right common iliac vein (RCIV), and LCIV. Visualization of 2 out of 3 locations is needed to define conservation of flow from the iliac veins into the IVC. If this is not feasible, the patient is excluded. Second, the sonographer begins acquiring velocity and area data. Three different acquisitions are made in the visible IVC, RCIV, and LCIV. Acquisitions consist of a five-second spectral Doppler waveform measuring velocity in the sagittal plane and a B-mode image measuring area in the transverse plane. Data is completed by acquiring three different acquisitions of velocity waveforms and area images in the right external iliac vein (REIV) and left external iliac vein (LEIV) (**Figure 2A**). The three acquisitions of velocity and area enable assessment of the degree of variability in the data. If large variations in the data are present, further acquisitions are made until consistent measurements are observed.

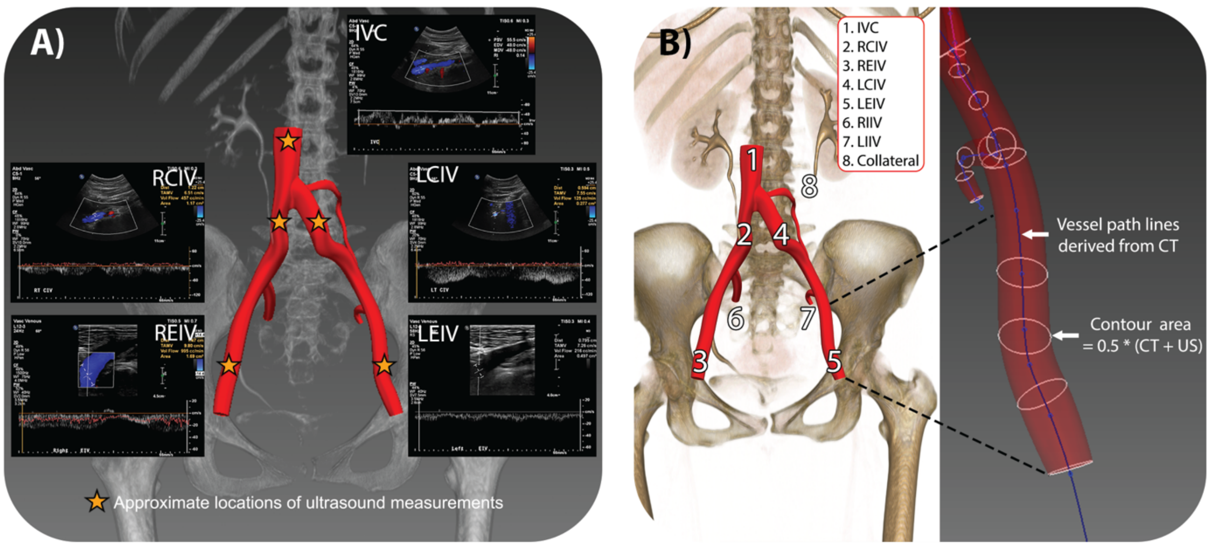

Figure 2. (A) Target locations for ultrasound measurements. (B) CT-derived path lines and contours. Contour area is adjusted to reflect confidence level in CT and ultrasound measurements. The figure shows an example where equal weights were given to the CT and ultrasound diameter data.

Computational Fluid Dynamics Simulations

Patient-specific computational models are created using the open-source blood flow modeling software CRIMSON[20]. CFD simulations require definition of i) the 3D geometry of the vessels of interest and ii) boundary conditions representing the inflow and outflow conditions of the different vessels.

<u>3D Patient-specific vascular geometries:</u> Geometric models of the iliac veins and IVC are constructed using CT and ultrasound data. Since values of vessel cross-sectional area are known to differ between US and CT[21,22], we have derived a geometric modeling protocol that enables

combining US and CT data to define vessel areas. First, vessel centerlines and contours are created using CT data. The CT-derived vessel contours can then be further adjusted using US data, to reflect the relative level of confidence between the CT and ultrasound imaging. In the example above, equal weight was given to CT and US to define vessel contour areas (**Figure 2B**).

<u>Inflow and outflow boundary conditions:</u> The US velocity data must be processed to i) extract flow data; ii) enforce conservation of flow across the inflow branches and IVC; and iii) define waveforms over the respiratory cycle. Towards that end, the following waveform adjustment protocol was developed (**Figure 3**).

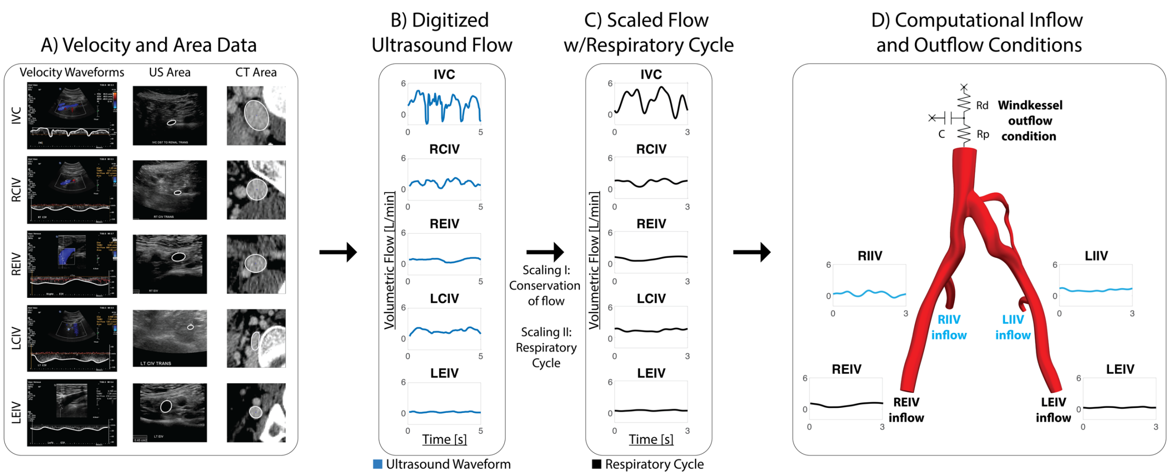

Figure 3. (A) Ultrasound velocity spectra are digitized and then multiplied by a weighted area of the US and CT data to create flow waveforms. (B) The flow waveforms are then twice scaled. The first scaling enforces conservation of flow (see equations 1-4). The second scaling sets a respiratory cycle while maintaining mean flow values. Lastly, respiratory cycles are smoothed out using a Fourier interpolation. (C) Internal iliac waveforms are estimated through point-by-point subtraction of the external iliac waveforms from the common iliac flow waveforms, then iteratively tuned to account for collateral flow. (D) Measured (REIV and LEIV) and estimated (RIIV and LIIV) flow waveforms are applied as inflow conditions to the computational model. A Windkessel model is tuned to accommodate the measured IVC outflow while setting a mean infrarenal IVC pressure of 10 mmHg (see equations 5-8).

i) Flow waveforms extraction: the contours of the five-second spectral Doppler velocity data for each vessel were digitized using the open-source Plot Digitizer (plotdigitizer.sourceforge.net) software. The contours represent the maximum velocity (V_{max}) in the Doppler spectrum. Assuming a parabolic velocity profile, mean velocities V_{mean} can be estimated as: $V_{mean} = 0.5 * V_{max}$. Mean velocities are then multiplied by a weighted area of the US and CT data to obtain flow waveforms (**Figure 3A**).

ii) Conservation of flow across branches: the ultrasound flow waveforms are scaled to enforce conservation of flow such that the sum of the inflows is equal to the IVC outflow. Here, two scenarios are possible:

1. If all three flow measurements are available $Q_{IVC}^{measured}$, $Q_{RCIV}^{measured}$, and $Q_{LCIV}^{measured}$, the measured IVC flow will generally not match the sum of RCIV and LCIV flows. Therefore, the following corrections are made. We first define a "calculated IVC flow" as:

   $$Q_{IVC}^{calculated} = Q_{RCIV}^{measured} + Q_{LCIV}^{measured} \tag{1}$$

   Next, a "corrected IVC flow" is defined as:

   $$Q_{IVC}^{corrected} = \frac{Q_{IVC}^{calculated} + Q_{IVC}^{measured}}{2} \tag{2}$$

   This correction represents a weighted average of the direct IVC flow measurement, and that given by the sum of RCIV and LCIV measurements. The following scaling factor for IVC flow is defined as:

   $$k_{IVC}^{scaling} = \frac{Q_{IVC}^{corrected}}{Q_{IVC}^{measured}} \tag{3}$$

   Finally, a scaling factor for the RCIV and LCIV flows is defined as:

   $$k_{branches}^{scaling} = \frac{Q_{IVC}^{corrected}}{Q_{IVC}^{calculated}} \tag{4}$$

   This scaling factor is also applied to the REIV and LEIV flow measurements.

2. If the sonographer was not able to visualize the IVC, RCIV, or LCIV, the missing vessel's flow is estimated by enforcing: $Q_{IVC} = Q_{RCIV} + Q_{LCIV}$.

iii) Respiratory cycle scaling: given that venous flows are greatly influenced by the respiratory cycle[10,23], the patient's respiratory rate is used to set a periodic cycle in the flow waveforms. The respiratory-adjusted waveforms are scaled such that their mean flows remained unchanged relative to the conservation-of-flow-adjusted waveforms. Lastly, the respiratory cycles are smoothed using an 8 mode Fourier interpolation (**Figure 3B)**.

Lastly, right internal iliac vein (RIIV) and left internal iliac vein (LIIV) waveforms are estimated through point-by-point subtraction of the external iliac waveforms from the common iliac waveforms (**Figure 3C)**. REIV, RIIV, LEIV, and LIIV waveforms are then applied as inflow boundary conditions at the model inlets. A Windkessel lumped-parameter model consisting of a proximal resistance (R_p), a capacitance (C), and a distal resistance (R_d) is coupled to the infrarenal IVC (**Figure 3D**). The sum of proximal and distal resistance is the total IVC resistance (R_T). The parameters are tuned so that the average pressure in the infrarenal IVC is 10 mmHg[24] while accommodating the measured IVC outflow (Equations 5-8), following an algorithm delineated by Xiao[25].

$$R_T = \frac{\text{Pressure}}{Flow} = \frac{10\,mmHg}{Flow_{IVC}} \tag{5}$$

$$R_p = 0.05 * R_T \tag{6}$$

$$R_d = 0.95 * R_T \tag{7}$$

$$C = \frac{(Flow_{IVC,MAX} - Flow_{IVC,MIN}) * \Delta t_{respiratory}}{2 * 10\,mmHg} \tag{8}$$

The vessel walls are modeled as rigid; therefore, a zero-velocity boundary condition was imposed. Blood is modeled as a non-Newtonian fluid[26], with viscosity defined by the Carreau-Yasuda model with parameters η_∞ = 0.0035 Pa·s, η_0 = 0.16 Pa·s, n = 0.2128, a = 0.64, and λ = 8.2

s [27]. Simulations of blood flow and pressure are performed in the Great Lakes high-performance computing cluster at the University of Michigan using 144 cores. The time step size is 0.0001 seconds. Simulations are run for 4 respiratory cycles, or until cycle-to-cycle periodicity is observed in IVC outflow. Mesh independence studies are performed for each subject, with finite element meshes consisting of 2, 4, and 8 million linear tetrahedral elements. Mesh independence was achieved for the 4 million element mesh, and therefore the results reported in this paper correspond to that level of mesh refinement.

Flow Calibration and Velocity Validation

Due to the lack of knowledge on flows through collateral vessels, and the discrepancies between area values between CT and US data, we propose an adjustment process for flows in internal iliac veins and cross-sectional areas of the common iliac veins as outlined in **Figure 4**.

Flow Calibration: discrepancies between simulated and computed common iliac vein flows may be observed. These are due to flow through collateral vessels which has not been explicitly accounted for in the strategy previously delineated. In that case, internal iliac waveforms are iteratively adjusted until the difference between measured and simulated common iliac vein flows is smaller than 3%.

Velocity Validation: because ultrasound velocity is the only direct hemodynamic measurement and the key quantity of interest to calculate shear rates, computational results are validated by comparing ultrasound velocities against simulated velocities. Simulated velocities are averaged in slices of the RCIV and LCIV. The location of each slice is set to the approximate location of the corresponding ultrasound measurement. The mean cross-sectional area of simulated velocities is averaged over the respiratory cycle and then compared to the mean ultrasound velocities. If percentage errors larger than 10% are observed, the area weighting given to define vessel contour areas using CT and US data is adjusted until a good agreement between simulated and measured velocities is achieved.

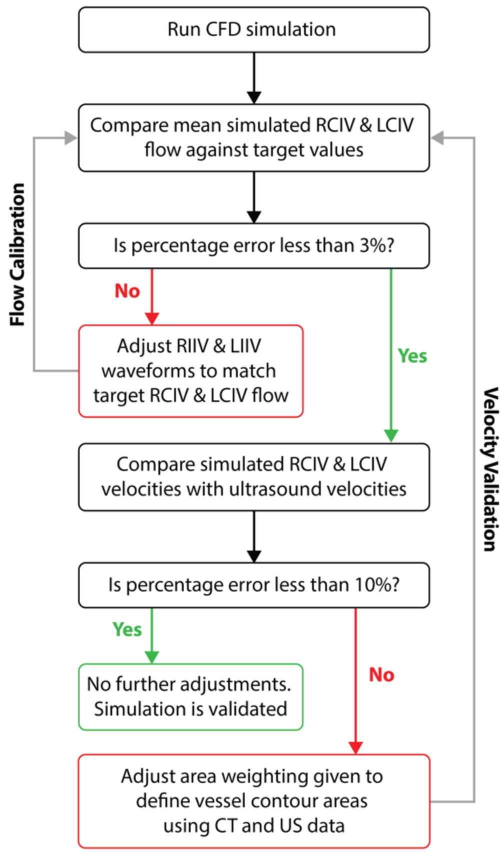

Figure 4. Adjustment process for internal iliac flow and cross-sectional areas of the common iliac veins. This strategy accounts for flow through collateral vessels and the discrepancies between area values in CT and US data.

Shear Rate Quantification

Shear rate is estimated thorough the von Mises criteria of the gradient of the velocity field[28]. Representative values of shear rates in the RCIV and LCIV were obtained by averaging the field of shear rates from the IVC bifurcation to the internal iliac bifurcation over the respiratory cycle. A one-sided, unpaired t test (α = 0.05) will be performed for the LCIV/RCIV shear rate ratios between the Subject group and the Control group to assess if IVCS compression leads to statistically significant changes in shear rates.

Results

The table below contains mean flows for each branch of the vascular model for 2 patients with IVCS (**Table I**). Due to collateral vessel flow, Patient 1 required adjustment of LIIV flow to match LCIV flow, whereas Patient 2 required adjustments of both LIIV and RIIV flows to match LCIV and RCIV flow. Furthermore, Patient 2 required adjustment of RCIV cross sectional areas to achieve good matching between measured and simulated velocities (**Figure 4**).

Table I. Mean flows (L/min) for Patients 1 & 2. Measured ultrasound flows (**Ultrasound**), respiratory-adjusted flow waveforms (**Scaled**), initial simulated flows (**Simulation**), and calibrated simulated flows (**Calibrated Simulation**) are displayed.

Patient 1

Vessel	Ultrasound	Scaled	Simulation	Calibrated Simulation
IVC	2.11	2.54	2.54	2.58
LCIV	1.6	1.36	1.32	1.36
RCIV	1.37	1.18	1.18	1.18
LEIV	0.37	0.32	0.32	0.32
REIV	0.92	0.82	0.82	0.82
LIIV	NA	1.04	1.04	1.08
RIIV	NA	0.36	0.36	0.36
Ipsilateral Collateral	NA	NA	0.04	0.04

Patient 2

Vessel	Ultrasound	Scaled	Simulation	Calibrated Simulation
IVC	1	0.82	0.82	0.84
LCIV	0.16	0.21	0.18	0.21
RCIV	0.4	0.61	0.63	0.61
LEIV	0.13	0.19	0.19	0.19
REIV	0.18	0.26	0.26	0.26
LIIV	NA	0.02	0.02	0.07
RIIV	NA	0.35	0.35	0.32
Ipsilateral Collateral	NA	NA	0.02	0.02
Paravertebral Collateral	NA	NA	0.03	0.03

Outflow RCR parameters were then tuned to achieve an average IVC pressure of 10 mmHg. The tuned parameters in mm·g·s base units are $R_p = 0.0016$, $C = 24.8$, and $R_d = 0.030$ for Patient 1 and $R_p = 0.0048$, $C = 24.8$, and $R_d = 0.092$ for Patient 2.

Figure 5A displays the validation of simulation velocities with ultrasound measurements. As stated earlier, the adjustment method outlined in **Figure 4**, discrepancies between simulated and measured velocities are smaller than 10%. **Figure 5B** displays representative volume renderings of velocity magnitude (mm/s) and shear rate (s^{-1}). For each patient, a summary of clinical history is delineated below.

Patient 1 is a 22-year-old female who presented with acute lower left extremity discomfort and a pulmonary embolus. The patient had a history of Factor V Leiden mutation and reported taking oral contraceptives, both known risk factors for DVT. Elevated shear rates were observed in the patient's left common iliac vein, with a mean shear rate of 122 $s^{-1}$and a peak shear rate of 1811 s^{-1}. Therefore, the LCIV/RCIV shear rate ratio for this patient was 2.0 for mean shear rate, and 2.1 for peak shear rate.

Patient 2 is a 40-year-old female with chronic DVT in the right and left lower extremities. Her DVT first presented after while pregnant in 2003. DVT re-presented while she was sick with COVID pneumonia in 2021. The patient had a history of Factor V Leiden Mutation and a family history of DVT, both known risk factors for DVT. Elevated shear rates were observed in the patient's left common iliac vein, with a mean shear rate of 180 s^{-1} and a peak shear rate of 922 s^{-1} and. Therefore, the LCIV/RCIV shear rate for this patient was 2.5 for mean shear rate and 0.9 for peak shear rate.

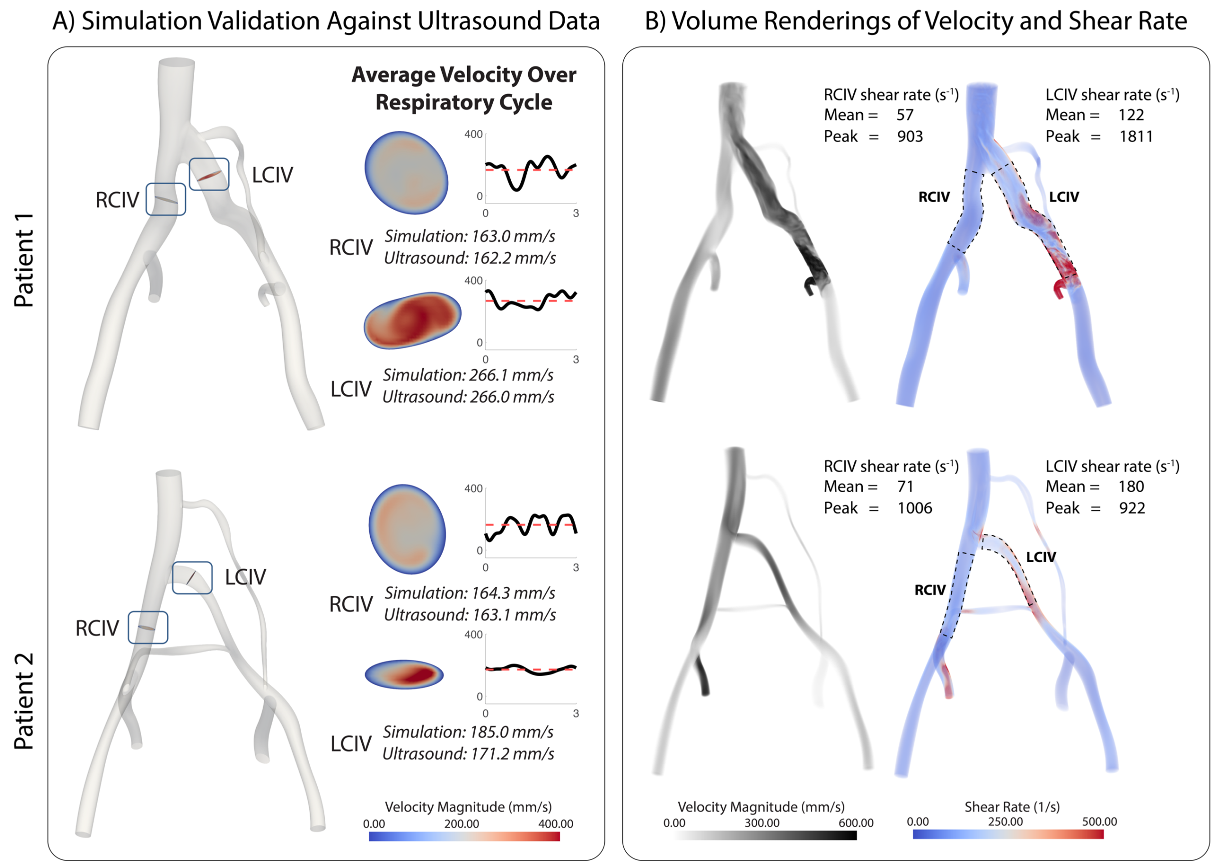

Figure 5. (A) To validate simulation results, slices are taken in the RCIV and LCIV corresponding to the approximate location of ultrasound measurements. Velocity is averaged in the slices over the respiratory cycle, then validated against average ultrasound velocity. Simulated and measured velocities agreed within 10%. (B) Volume-renderings of velocity and shear rate are displayed for two patients. Peak and mean shear rates in the RCIV and LCIV are displayed. Elevated LCIV shear rates were observed for both patients.

Discussion

The accepted treatment for thrombotic IVCS patients is to lyse the clot and stent the underlying iliac vein stenosis[2]. For non-thrombotic IVCS patients, there is significant variability in clinical management, especially for mild symptoms of venous insufficiency. Some physicians will treat conservatively with compression stockings and/or anticoagulant therapies, whereas other physicians treat aggressively by stenting the compressed vein[29]. Differences in interpretation of the available imaging and hemodynamic data may lead to the differences in treatment approaches.

The purpose of this protocol is to standardize venous hemodynamic evaluation of patients with IVCS. Results reported here have revealed that IVCS patients may experience elevated shear rates, with peak shear rates reaching over 1000 s^{-1} (**Figure 5B**). As a single-center, nonrandomized, case-control study, generalizability of results may be limited. This will require replication at other centers and patient populations. Larger patient cohorts will be investigated to help establish whether high shear rates could be a potential contributing mechanism for thrombosis initiation in IVCS patients. Furthermore, CFD analyses could provide insights into which patients would benefit from stenting versus conservative treatment.

Visualizing the IVC and common iliac veins during ultrasound imaging may be challenging due to vessel motion during breathing, bowel gas, and body habitus. These challenges were addressed by instructing the patient to breathe normally and not to eat solid foods prior to the scan. We found that deep inspiration or expiration caused the IVC and common iliac veins to move, making ultrasound acquisitions difficult for the sonographer. Instructing the patient to breathe normally circumvented this issue. Future work could examine the effects of deep inspiration and expiration on venous hemodynamics via intravascular ultrasound (IVUS). Furthermore, instructing the patient not to consume solid foods for at least 8 hours before the scan reduces the amount of bowel gas, improving visualization of the IVC, RCIV, and LCIV greatly. However, hydration status is important for blood volume and may affect hemodynamics measured via ultrasound[10]. Thus, to ensure that ultrasound measurements are representative of the patient's typical venous hemodynamics, we recommend instructing the patient to drink oral fluids as usual prior to the ultrasound scan.

Despite the improved visualization from not consuming solid food, the depth of the IVC, RCIV, and LCIV can potentially make data acquisition difficult for the sonographer. To reduce scan time, ultrasound data acquisition is split into a location phase and an acquisition phase. If the sonographer cannot visualize at least 2 out of the IVC, LCIV, and RCIV, then the patient is excluded from the study before any images are acquired. This reduces the scan from 20 minutes to less than 5 minutes if the patient cannot be well-visualized.

While post-processing ultrasound and CT data, ultrasound area measurements were observed to differ from CT area measurements sometimes by over 100%. These discrepancies are due to several reasons, such as the ultrasound and CT scans are not performed on the same day, as well as the impact of the patient's hydration status on vessel cross-sectional area[10]. Additionally, because patients with chronic DVT typically undergo a cycle of thrombus formation and resolution[30], the timing of each scan in the DVT formation-resolution cycle will impact observed hemodynamics. For example, if a patient is imaged with a partially occluding LCIV thrombus, the increased resistance from the thrombus will divert flow to the collateral veins and thus decrease LCIV shear rate. Conversely, if the patient is imaged with no LCIV thrombus, less flow will be diverted to collateral vessels and higher LCIV shear rates will be observed. In the results presented, both patients were imaged with no thrombus present. The calculated shear rates were consistent with their observed clinical symptoms. Patient 1, with a history of left lower extremity symptoms, has elevated peak shear rates in the LCIV. Patient 2, with a history of bilateral thrombosis, has elevated peak shear rates in both the RCIV and LCIV.

Depending on the level of confidence in the data, area weighting can be adjusted in the model to favor CT or ultrasound measurements. Furthermore, velocity and area measurements can vary within the same scan depending on the pressure applied by the sonographer and the angle of interrogation used to visualize veins. To verify that velocity and area measurements are precise, we recommend taking at least 3 images of each measurement at each location. Efforts were also made to keep the angle of interrogation under 60 degrees. Furthermore, the exclusion criteria for patients whose iliac veins cannot be well-visualized via ultrasound favors lower BMI, as increased body habitus makes visualization of the IVC and common iliac veins via duplex ultrasound more difficult. Obtaining velocity and area measurements via IVUS may be superior to duplex ultrasound in patients with larger body habitus, however IVUS is invasive and presents limitations such as imaging artifacts from shadowing, guidewires, and air bubbles[31].

The uncertainties in area and velocity measurements manifest in the computational model's inflow waveforms. Alternative techniques, such as Kripfgans' method of surface integration of velocity vectors[11], could be used to create the model's inflow waveforms. Furthermore, our computational models are run under rigid anatomical conditions, whereas veins can have large variations in cross-sectional area. Physiologically, the LCIV behaves as a semi-rigid vessel due to its compression by the right common iliac artery and the lumbar spine[32], thus our simulations should reasonably estimate LCIV shear rate. The simulation, however, may overestimate the RCIV shear rates due to vessel expansion during peak flow, decreasing the velocity gradient. This leads to an underestimation of the LCIV/RCIV shear rate ratio and serves as a limitation to the present study. Future work could examine the effects of vessel wall motion on venous hemodynamics in the iliac veins.

Acknowledgements

Computing resources were provided by NSF Grant-1531752.

References

1. May R, Thurner J. The Cause of the Predominantly Sinistral Occurrence of Thrombosis of the Pelvic Veins. Angiology [Internet]. 1957 Oct 1;8(5):419–27. Available from: https://doi.org/10.1177/000331975700800505

2. Peters M, Syed RK, Katz M, Moscona J, Press C, Nijjar V, et al. May-Thurner Syndrome: A Not So Uncommon Cause of a Common Condition. Baylor Univ Med Cent Proc. 2012;25(3):231–3.

3. Brotman DJ, Deitcher SR, Lip GYH, Matzdorff ACBT-SMJ. Virchow’s triad revisited. 2004 Apr 13;97(2):213+. Available from: https://link.gale.com/apps/doc/A114134751/AONE?u=umuser&sid=googleScholar&xid=fa2b3b0f

4. Kaltenmeier CT, Erben Y, Indes J, Lee A, Dardik A, Sarac T, et al. Systematic review of May-Thurner syndrome with emphasis on gender differences. J Vasc Surg Venous Lymphat Disord [Internet]. 2018;6(3):399-407.e4. Available from: https://doi.org/10.1016/j.jvsv.2017.11.006

5. Jayaraj A, Buck W, Knight A, Johns B, Raju S. Impact of degree of stenosis in May-Thurner syndrome on iliac vein stenting. J Vasc Surg Venous Lymphat Disord [Internet]. 2019;7(2):195–202. Available from: https://doi.org/10.1016/j.jvsv.2018.10.001

6. Rosendaal FR. Venous thrombosis: a multicausal disease. Lancet (London, England). 1999 Apr;353(9159):1167–73.

7. Mehta JL, Calcaterra G, Bassareo PP. COVID-19, thromboembolic risk, and Virchow’s triad: Lesson from the past. Clin Cardiol. 2020;43(12):1362–7.

8. Sakariassen KS, Orning L, Turitto VT. The impact of blood shear rate on arterial thrombus formation. Futur Sci OA. 2015;1(4).

9. Ruggeri ZM. The role of von Willebrand factor in thrombus formation. Thromb Res. 2007;120(SUPPL. 1):1–10.

10. Meissner MH, Moneta G, Burnand K, Gloviczki P, Lohr JM, Lurie F, et al. The

hemodynamics and diagnosis of venous disease. J Vasc Surg. 2007;46(6 SUPPL.):4–24.

11. Kripfgans OD, Rubin JM, Hall AL, Gordon MB, Fowlkes JB. Measurement of volumetric flow. J Ultrasound Med. 2006;25(10):1305–11.

12. Figueroa CA, Taylor CA, Marsden AL. Blood Flow. In: Stein E, de Borst R, Hughes TJR, editors. Encyclopedia of Computational Mechanics. Second. John Wiley & Sons; 2017.

13. Taylor CA, Figueroa CA. Patient-specific Modeling of Cardiovascular Mechanics. 2015;33(4):395–401.

14. Ahmed Y, Tossas-Betancourt C, van Bakel PAJ, Primeaux JM, Weadock WJ, Lu JC, et al. Interventional Planning for Endovascular Revision of a Lateral Tunnel Fontan: A Patient-Specific Computational Analysis. Front Physiol. 2021;12(August):1–11.

15. van Bakel TMJ, Lau KD, Hirsch-Romano J, Trimarchi S, Dorfman AL, Figueroa CA. Patient-specific modeling of hemodynamics: Supporting surgical planning in a fontan circulation correction. J Cardiovasc Transl Res. 2018;11(2):145–55.

16. Van Bakel TM, Arthurs CJ, Van Herwaarden JA, Moll FL, Eagle KA, Patel HJ, et al. A computational analysis of different endograft designs for Zone 0 aortic arch repair. Eur J Cardio-thoracic Surg. 2018;54(2):389–96.

17. Baliyan V, Shaqdan K, Hedgire S, Ghoshhajra B. Vascular computed tomography angiography technique and indications. Cardiovasc Diagn Ther. 2019;9(S1):S14–27.

18. Youn YJ, Lee J. Chronic venous insufficiency and varicose veins of the lower extremities. Korean J Intern Med. 2019;34(2):269–83.

19. Needleman L, Cronan JJ, Lilly MP, Merli GJ, Adhikari S, Hertzberg BS, et al. Ultrasound for lower extremity deep venous thrombosis: Multidisciplinary recommendations from the society of radiologists in ultrasound consensus conference. Circulation.

2018;137(14):1505–15.

20. Arthurs CJ, Khlebnikov R, Melville A, Marčan M, Gomez A, Dillon-Murphy D, et al. CRIMSON: An open-source software framework for cardiovascular integrated modelling and simulation. PLoS Comput Biol. 2021;17(5):1–20.

21. Toh MR, Damodharan K, Lim M, Yap C, Chong TT, Tang TY. Computed tomography venography versus intravascular ultrasound in the diagnosis of iliofemoral vein stenosis. J Vasc Surg Venous Lymphat Disord [Internet]. 2020;8(6):1122–3. Available from: http://dx.doi.org/10.1016/j.jvsv.2020.07.014

22. Han SM, Patel K, Rowe VL, Perese S, Bond A, Weaver FA. Ultrasound-determined diameter measurements are more accurate than axial computed tomography after endovascular aortic aneurysm repair. J Vasc Surg [Internet]. 2010;51(6):1381–9. Available from: http://dx.doi.org/10.1016/j.jvs.2010.01.033

23. Moneta GL, Bedford G, Beach K, Strandness DE. Duplex ultrasound assessment of venous diameters, peak velocities, and flow patterns. J Vasc Surg. 1988;8(3):286–91.

24. Tedaldi E, Montanari C, Aycock KI, Sturla F, Redaelli A, Manning KB. An experimental and computational study of the inferior vena cava hemodynamics under respiratory-induced collapse of the infrarenal IVC. Med Eng Phys [Internet]. 2018;54:44–55. Available from: https://doi.org/10.1016/j.medengphy.2018.02.003

25. Xiao N, Alastruey J, Figueroa CA. A systematic comparison between 1-D and 3-D hemodynamics in compliant arterial models. Int j numer method biomed eng [Internet]. 2014 Feb [cited 2022 Oct 4];30(2):204–31. Available from: https://pubmed.ncbi.nlm.nih.gov/24115509/

26. Lynch S, Nama N, Figueroa CA. Effects of non-Newtonian viscosity on arterial and

venous flow and transport. Sci Rep [Internet]. 2022;12(1):20568. Available from: https://doi.org/10.1038/s41598-022-19867-1

27. Abraham F, Behr M, Heinkenschloss M. Shape optimization in steady blood flow: A numerical study of non-Newtonian effects. Comput Methods Biomech Biomed Engin [Internet]. 2005 Apr 1;8(2):127–37. Available from: https://doi.org/10.1080/10255840500180799

28. Mises R v. Mechanik der festen Korper im plastisch- deformablen Zustand. Available from: https://www.digizeitschriften.de/id/252457811_1913%7Clog53

29. Hng JZK, Su S, Atkinson N. May–Thurner syndrome, a diagnosis to consider in young males with no risk factors: a case report and review of the literature. J Med Case Rep [Internet]. 2021;15(1):1–7. Available from: https://doi.org/10.1186/s13256-021-02730-8

30. Meissner MH, Caps MT, Bergelin RO, Manzo RA, Strandness DEJ. Propagation, rethrombosis and new thrombus formation after acute deep venous thrombosis. J Vasc Surg. 1995 Nov;22(5):558–67.

31. McLafferty RB. The role of intravascular ultrasound in venous thromboembolism. Semin Intervent Radiol. 2012;29(1):10–5.

32. Zucker EJ, Ganguli S, Ghoshhajra BB, Gupta R, Prabhakar AM. Imaging of venous compression syndromes. Cardiovasc Diagn Ther. 2016;6(6):519–32.